NOWPAP CEARAC

Northwest Pacific Action Plan
Special Monitoring and Coastal Environmental Assessment
Regional Activity Centre

5-5 Ushijimashin-machi, Toyama City, Toyama 930-0856, Japan
Tel: +81-76-445-1571, Fax: +81-76-445-1581
Email: webmaster@cearac.nowpap.org
Website: https://cearac.nowpap.org

Report on Assessment of the Distribution of Tidal Flats in the NOWPAP Region

NOWPAP CEARAC 2022

Published in 2022
by the NOWPAP Special Monitoring and Coastal Environmental Assessment Regional Activity Centre (NOWPAP CEARAC)
Established at the Northwest Pacific Region Environmental Cooperation Center
5-5 Ushijimashin-machi, Toyama City, Toyama 930-0856
E-mail: cearac@npec.or.jp
Website: https://cearac.nowpap.org

For bibliographic purposes this document should be cited as: NOWPAP CEARAC, 2022. Report on Assessment of the Distribution of Tidal Flats in the NOWPAP Region

Photos of tidal flats in Korea were provided by Jongseo YIM

Contributing Experts

Dr. Jie SU
Lab of Marine Ecology
National Marine Environmental Monitoring Center, China

Dr. Jongseo YIM
Korea Maritime Institute, Korea

Dr. Kirill BAZAROV
Pacific Geographical Institute, Russia

Dr. Nicholas MURRAY
College of Science and Engineering
James Cook University, Australia

Dr. Takafumi YOSHIDA
CEARAC Secretariat

Table of Contents

1. Background and objectives

1.1 Tidal flats and salt marshes in the NOWPAP region

In the northwest Pacific (NOWPAP) region, there are tidal flats spread over wide areas, especially in the coastal sea areas of China, Japan, and Korea. Areas around the Yellow Sea are the main locations where tidal flats are distributed. On the western coast of Korea and around the Shandong Peninsula of China, there are huge stretches of tidal flats. In Japan, major distribution areas are located near the Ariake Sea and the Seto Inland Sea. On the other hand, in the northern part of the NOWPAP region, including Russian waters, the tide is quite weak and some small-scale tidal flats are distributed along the Tatar Strait.

There are many kinds of marine species, including benthic species such as bivalves, crustaceans, and fish using the tidal flats, and some of them are listed as endangered species in the member states. The horseshoe crab (*Tachypleus tridentatus*) and Bluespotted Mud Hopper (*Boleophthalmus pectinirostris*) are categorized as endangered (EN), and the fiddler crab (*Uca arcuata*) is categorized as vulnerable (VU) in Japan. In the NOWPAP region, tidal flats are important sites for migratory birds. The northwest Pacific region is located in the East Asian-Australian Flyway, and 250 kinds of migratory birds fly between Australia and the Russian Far East. During migration, birds use the wetlands for resting and feeding. Thirty-six species of migratory birds using the East Asian-Australian Flyway are globally threatened species. The Great Knot (*Calidris tenuirostris*), Far Eastern Curlew (*Numenius madagascariensis*), Spoon-billed Sandpiper (*Calidris pygmaea*), and Spotted Greenshank (*Tringa guttifer*) are among those designated as endangered.

Salt marshes are also important coastal habitats. Information, however, on the distribution of salt marshes in the NOWPAP region is quite limited compared with that available regarding tidal flats. The UN Environment Programme World Conservation Monitoring Centre provides information about the global distribution of salt marshes (https://data.unep-wcmc.org/datasets/43) (Figure 1), and the distribution map shows extensive salt marsh coverage along Chinese coastal lines. Yang and Chen (1995) reported there are 56,680 ha of salt marshes in the coastal areas of China. There are a few salt marsh sites in Japan, Korea, and Russia as well.

Figure 1. Distribution of salt marshes in the Northwest Pacific region.
(UN Environment Programme World Conservation Monitoring Centre)

1.2 Anthropogenic impact on tidal flats and salt marshes in the NOWPAP region

Over the past 50 years, large areas of coastal wetlands have been lost in the NOWPAP region: 51% in China, 40% in Japan, and 60% in Korea (MacKinnon et al., 2012). Member states in the region have long histories of coastal development, and this is one of the main causes of decreasing coastal wetlands, including tidal flats and salt marshes.

The Data and Information Network Regional Activity Centre (DINRAC) of NOWPAP implemented an activity concerning the sea reclamation state and management project in the NOWPAP region in the 2018-2019 biennium. Past sea reclamations in the NOWPAP member states were summarized (NOWPAP DINRAC, 2021). In China, the oldest record of sea reclamation dates back to the Han Dynasty, 2000 years ago. Recent active reclamations started in the 1950s for disaster prevention, agricultural reclamation, and salt drying. In the 1960s to 1970s, reclamation projects were conducted for creating agricultural land, in the 1980s to 1990s for developing aquaculture ponds, and in the 2000s with rapid economic growth. By the end of the last century, the total reclamation area was 1.2 million ha, and 49% of tidal flats were lost over the last three decades (from 4,992 to 2,547 km^2) (Chen et al., 2019). In Japan, one of the oldest records on reclamation dates back to the late 13th century, around the Ariake Sea. More recently, huge coastal developments including landfills and land reclamation projects were conducted there in the 1920s-1940s. To create agricultural and industrial zones, many tidal flat areas were diked and lost. As shown in Figure 2, the current total area of tidal flats in the Seto Inland Sea is half of the total area present in the 18th century. Reclamation projects in Korea have been conducted since the Goryeo Dynasty (918-1392) for developing agricultural land. In the 1980s, large-scale reclamations were implemented to meet needs for additional land not only for agricultural activities but also urbanization, with construction of industrial complexes, ports, power generation facilities, and environmental pollution treatment facilities. In 1964, the total area of tidal flats was 3,905 km^2. However, the total area was half of this amount by the beginning of the 2000s.

In Russia, there is no available information on past coastal development in or around tidal flats.

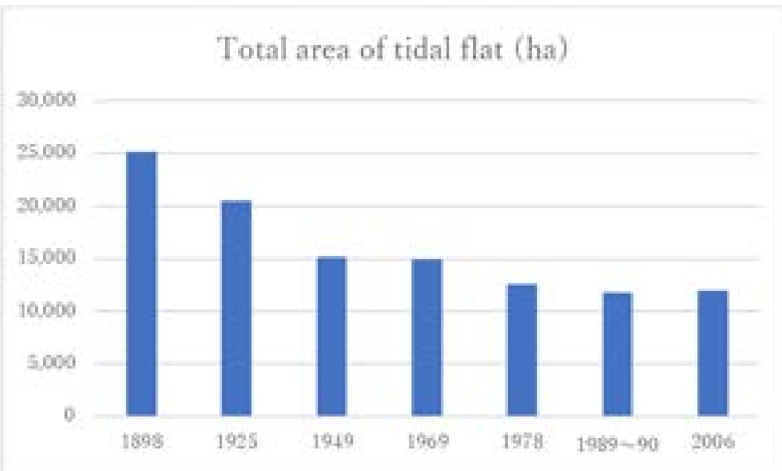

Figure 2. Historical change of the total area of tidal flats in the Seto Inland Sea, Japan.

1.3 CEARAC Medium-term Strategy for marine biodiversity conservation

CEARAC started its activities on marine biodiversity conservation in 2010. At the beginning, CEARAC aimed to collect information on national actions for marine biodiversity conservation in the member states to share within the region. At the 10th meeting of the Conference of the Parties to the Convention on Biological Diversity (COP10), the Strategic Plan 2011-2020, including Aichi Biodiversity Targets, was adopted. In this plan, Target 11 in particular aimed to protect 10% of coastal and marine area as Marine Protected Areas (MPA). Thus, CEARAC shifted its focus to marine protected areas (MPAs) and sources of pressure on marine biodiversity in the NOWPAP region, implementing new projects and publishing several useful reports.

Following a request in 2017 by CEARAC Focal Points (FPs) for a clearer future vision on how CEARAC can contribute to marine biodiversity conservation in the NOWPAP region, the CEARAC Secretariat developed the CEARAC Medium-term Strategy for Marine Biodiversity Conservation (MTS BIO) in 2019. This MTS BIO is CEARAC's strategic document stating its basic policy, future vision, and direction. It also outlines the priority of topics CEARAC should implement in the future for marine biodiversity conservation in the NOWPAP region while pursuing its mandates of development of coastal environmental assessment tools using special monitoring techniques, as well as assessment of the marine environment in the NOWPAP region with the assessment tools developed since its establishment in 2002.

In the MTS BIO, conservation of biological habitats including tidal flats, salt marshes, and seagrass/seaweed beds in the NOWPAP region is selected as a highly prioritized topic. Seagrass and seaweed are distributed widely throughout the NOWPAP region, serving as significant coastal habitats for marine species. In addition, seagrass/seaweed beds are important for the absorption of CO2, namely blue carbon. CEARAC has thusly implemented projects to map seagrass bed distribution using remote sensing techniques since 2014. Using accumulated experience in coastal monitoring using satellites, CEARAC developed a manual for mapping seagrass/seaweed distribution in 2015 with support of experts from the NOWPAP member states, and conducted the assessment of seagrass distribution with a manual developed over the following biennia. CEARAC also developed a cloud-based tool, the Seagrass Mapper, for mapping seagrass distribution using satellite images. The Seagrass Mapper is available through the Mapseagrass Project website (https://mapseagrass.org/), one of the CEARAC's website for mapping seagrass.

1.4 Objectives of this project

While seagrass/seaweed beds are a significant habitat in water in the NOWPAP region, tidal flats and salt marshes are significant on land, both serving important, irreplaceable roles in marine biodiversity conservation. In the coastal areas of NOWPAP member states, wide tidal flats areas are distributed and provide ecosystem services to human and marine species. Due to coastal development, however, these precious habitats have lost area over the past several decades. It is necessary to understand negative impacts in the past and to protect/restore the remaining tidal flats/salt marshes for the future. The CEARAC Secretariat therefore proposed a new project, the “Assessment of the distribution of tidal flats and salt marshes in the NOWPAP region,” at the 17th CEARAC FPM in 2018, and it was approved by CEARAC FPs.

The objective of this project is to understand the current status of and historical changes in tidal flats/salt marshes in the NOWPAP region by mapping the past and current tidal flats/salt marshes using remote sensing images. Unfortunately, as available data on salt marshes in the NOWPAP regions of the member states remains quite limited, tidal flats are the main target habitat in this project.

Remote sensing is a very useful monitoring tool for marine environments. Satellite images are influenced strongly by weather conditions, such as clouds. They can, however, provide snapshots of wide-scale areas where conventional ship observation cannot cover at once, and provide regular monitoring results. In the 1980s, scientific analysis with satellite images was not as reliable as now, so it was difficult to apply remote sensing techniques to monitoring of habitat changes. However, in recent years, satellite images such as MODIS, Landsat, and Sentinel are available free of charge, and high-grade computers are available for analyzing large-scale data. In addition, thanks to the development of cloud computing in recent years, it became possible to analyze larger numbers of satellite images. Using such useful state-of-the-art tools and technology, land use and coastal habitats are now being monitored in many regions around the world.

When CEARAC developed a manual for mapping seagrass/seaweed distribution in the NOWPAP region, it took a great deal of time, money, and support from experts because there were no tools to suit the objectives of the CEARAC’s project. It was therefore necessary to apply existing tools for tidal flat monitoring, and Dr. Nicholas Murray from James Cook University in Australia has developed a global mapping tool for tidal flats (Global Intertidal Change: GIC). On November 19, 2019, CEARAC organized a workshop with experts nominated from NOWPAP member states, inviting Dr. Murray to share his experiences while discussing how to map tidal flat distribution in the NOWPAP region. After reviewing the feasibility of using the GIC in CEARAC’s new project, members at the meeting agreed on adopting it in the NOWPAP region and the CEARAC Secretariat developed a workplan regarding implementation of this activity for the 2020-2021 biennium.

As the GIC aims to map the global distribution of tidal flats, upgrade of the GIC became necessary to suit the NOWPAP regional environments. CEARAC subsequently prepared a detailed implementation plan to upgrade the GIC based on newly added training dataset (information on the real distribution of tidal flats in NOWPAP member states) for mapping distribution. After the implementation plan was reviewed by the CEARAC FPs and approved in September 2020, the CEARAC Secretariat made a contract with James Cook University (Dr. Nicholas Murray) and the nominated experts from NOWPAP member states (Table 1) in order to develop a tidal flat distribution map in the NOWPAP region.

Table 1. Experts nominated for collecting information on tidal flats in each member state.

Country	Name of expert	Affiliation
China	Dr. Jie SU	National Marine Environment Monitoring Center
Japan	CEARAC Secretariat	
Korea	Dr. Jongseo YIM	Korea Maritime Institute
Russia	Dr. Kirill BAZAROV	Pacific Geographical Institute

1.5 Contribution to NOWPAP's actions for marine biodiversity conservation

NOWPAP plans to develop a Regional Action Plan for Marine and Coastal Biodiversity Conservation (RAP BIO) with a clear vision and direction on marine and coastal biodiversity conservation in the NOWPAP region, outlining roles and responsibilities of the member states and respective Regional Activity Centres (RACs). The first draft of the RAP BIO was prepared in 2021 in cooperation with an international consultant, NOWPAP RCU, all RACs, and national experts from the member states. The draft RAP BIO has been reviewed by the member states, and it is expected to be adopted as soon as possible.

The goal of RAP BIO is to strengthen cooperation and capacity building among the member states regarding conservation of marine and coastal biodiversity through generating and sharing information and analysis of the statuses of and trends in biodiversity and ecosystem services. RAP BIO promotes several indicative activities, one being "generating information on the status, trends, location, extent, and restoration needs of important habitats and critical ecosystems including tidal flats, salt marshes, and seagrass/seaweed beds in the NOWPAP region, including the use of habitat mapping tools." Thus, CEARAC's activities on coastal habitat mapping will be able to contribute to implementation of RAP BIO.

The Pollution Monitoring Regional Activity Centre (POMRAC) of NOWPAP developed Ecological Quality Objectives (EcoQOs) in 2014 and established a future desirable good environmental status in the NOWPAP region. Plans have been made to monitor the latest progress for achieving the good environmental status using the selected indicators, and one of the five EcoQOs is stated as "Biological and habitat diversity are not changed significantly due to anthropogenic pressure," so the diversity of marine mammals and water birds and the distribution of benthic and pelagic communities and their statuses are potential operational criteria under this EcoQO. CEARAC's coastal habitat mapping projects can provide useful information in understanding the current status of EcoQOs in the NOWPAP region.

2. Methodology

2.1 Introduction of Global Intertidal Change

Monitoring of tidal flats was conducted by in-situ monitoring in past surveys; in-situ monitoring, however, requires a huge amount of manpower and time to measure the extensive size of tidal flats. Since the 1980s, satellite images have been available free of charge, and higher-resolution satellite images have become available in recent years. These technological advancements help researchers survey environments in categories such as land-use and throughout various habitats. Since the 2010s, satellite images have become increasingly utilized for monitoring coastal environments.

For the sake of understanding the distribution of and changes in tidal flats, Murray et al. (2014) tried to assess the rapid loss of tidal wetlands in the Yellow Sea using satellite images. In the assessment, they used Landsat satellite images and classified tidal flats with images of low and high tide stages. Using the limited number of satellite images, they showed historical changes between the 1950s, 1980s and 2000s, and estimated the rapid loss of tidal flats in coastal areas of China and Korea.

In recent years, a new classification method was developed using big data and machine learning, enabling researchers to map distribution more easily. GIC was developed as one of the tidal flat distribution mapping tools by Dr. Nicholas Murray and his team (Murray et al., 2019). This approach is the first for mapping tidal flat distribution using satellite images from around the world. The GIC methodology for mapping tidal flats is actually a combination of remote-sensing classification and machine learning. By using the Google Earth Engine, a cloud-based analysis platform, it is possible to analyze a huge number of satellite images and detect the distribution of tidal flats using a random forest classification algorithm. This method of mapping tidal flats is briefly explained in the following section. More detailed information regarding the methodology is available in Dr. Murray's paper, "The global distribution and trajectory of tidal flats" (Murray et al., 2019).

(1) Classification approach for satellite images

Over 7,000,000 satellite images in the Landsat archives, which cover all global coastlines between 60ºN and 60ºS from 1984 to 2016, were analyzed to develop global maps of tidal flats. With the machine-learning classification model (random-forest classification algorithm), every 30-m pixel across global coastal zones were classified into three mapping classes: 'tidal flat,' 'permanent water,' and 'other.' This supervised machine-learning model was trained using input data from dense stacks of Landsat archive images, along with covariates from several other data layers that represent physical environments on the Earth's surface (global-scale bathymetry data, multiple Landsat-derived spectral reflectance variables, etc.). The final dataset consists of 11 global maps of tidal flats at 30-m pixel resolution for set time periods: 1984-1986, 1987-1989, 1990-1992, 1993-1995, 1996-1998, 1999-2001, 2002-2004, 2005-2007, 2008-2010, 2011-2013, and 2014-2016.

(2) Validation

Validation of the global dataset was conducted using an independent accuracy assessment approach. 1,358 random samples were selected for the validation and analyzed using an online validation application in Google Earth Engine. The validation application enabled three experienced independent analysts to concurrently annotate each sample to classify it as either a 'tidal flat' or 'other.' The application also enabled each analyst to assign a class to each sample with direct reference to (i) high-resolution Google Earth imagery, (ii) the Landsat OLI near-infrared band, (iii) a Landsat OLI true-color composite, (iv) a Landsat OLI false-color image composite, (v) an image composite representing the standard deviation of the NDWI (the normalized differenced water index), and (vi) an image composite representing the standard deviation of the AWEI (the automated water extraction index).

A standard remote-sensing error matrix approach indicated that the overall map accuracy was 82.3%.

(3) Definition of tidal flats

Generally, a tidal flat area is referred to as the whole area between the high tide line and the low tide line. In a paper published in 2014 by Murray et al., satellite images of high and low tides were used to show near-real distribution with a limited number of images. On the other hand, GIC aims to detect the distribution of tidal flats world-wide using machine learning in the method described in section 3.1, which has benefit of understanding distribution more easily and over wider areas. Therefore, it is said the definition (covered area) of tidal flat in GIC is different from the traditional definition. In fact, some NOWPAP member states monitor tidal flats using information on high/low tides, and they provide this data as national monitoring data. Thus, it is estimated that there are large differences between the tidal flat distribution provided by GIC and national data in these member states.

2.2 Error assessment of GIC: comparison between GIC data and real distribution in member states

For mapping tidal flats in the NOWPAP region, use of GIC was agreed upon at the workshop held in November 2019. GIC is the only tool available at present to map the global and regional distribution of tidal flats and their historical changes. However, as mentioned in the section above, it is estimated that GIC has several limitations in detecting tidal flats. First, GIC uses satellite images from Landsat, the resolution of which is 30 m, so it is difficult to detect small-scale tidal flats of less than 10 m in size. GIC also uses a machine-learning classification model using Google Earth Engine. This means that each pixel of a satellite image is classified into the three classes of tidal flats, permanent water, or other, using a random-forest classification algorithm. The random-forest classification algorithm detects tidal flats using high-spatial-resolution satellite imagery, global-scale bathymetry data, multiple Landsat-derived spectra, reflectance variables, and image time-series data from Google Earth and

Landsat. With this technology, point locations along the global coastline are confirmed as tidal flat ecosystems. Therefore, if there is not enough in-situ data (training data) and the sea area is covered with turbid water, detection errors may happen. Finally, definitions of tidal flats in GIC monitoring and national monitoring are different. This causes differences in terms of location and size of tidal flat distributions in the NOWPAP region.

To understand the limitations of GIC and improve on these points for the NOWPAP region, error assessments have been implemented using national monitoring data provided from each member state.

[China]

Information on tidal flat distribution in the Yellow River estuary and along the northern Yellow Sea near Liaoning Province was provided as national data (Figure 3). Differences between the national data provided and the tidal flats detected by GIC were then analyzed.

Figure 3. Distribution of tidal flats in the Yellow River estuary and the along the northern Yellow Sea near Liaoning Province.

Table 2. Comparison of the total area of tidal flats between national monitoring data and GIC data in China.

Sea area	*Area (ha)*			*Overlapped ratio (%)*
	National data	GIC	Overlapped	
North Yellow Sea	27,484	45,752	22,384	81.4
Yellow River Estuary	53,914	40,351	18,242	33.8

Table 3. Detailed information on differences in national monitoring data (ND) and GIC detection of tidal flats in the northern Yellow Sea.

	National Data	GIC
Number of meshes	185	7,561
Total Area of tidal flats (ha)	27,484	45,752
Number of overlapped meshes	146	
Total overlapped area (ha)	22,384	
Overlapped ratio (%) (Overlapped area/Total area of ND)	81.4	
Overlapped ratio (%) (Num. of overlapped meshes/meshes of ND)	78.9	
Mis-detection ratio (%) (Un-overlapped area/Total area of ND)	51.1	

Table 4. Detailed information on differences between national monitoring data (ND) and GIC detection of tidal flats in the Yellow River estuary.

	National Data	GIC
Number of meshes	5	3,558
Total Area of tidal flats (ha)	53,914	40,351
Number of overlapped meshes	5	
Total overlapped area (ha)	18,242	
Overlapped ratio (%) (Overlapped area/Total area of ND)	33.8	
Overlapped ratio (%) (Num. of overlapped meshes/meshes of ND)	100	
Mis-detection ratio (%) (Un-overlapped area/Total area of ND)	54.8	

Table 2, 3, and 4 show comparison results between the national data and GIC data. In the north Yellow Sea, GIC can detect tidal flats with high accuracy. The total area detected by the GIC is larger than that provided in the national data. Mis-detection by GIC reaches 23,000 ha, so improving the over-estimation of GIC will contribute to producing a more highly accurate map. On the other hand, accuracy is lower in the estuary of the Yellow River. The Yellow River is famous for discharging highly turbid water. As GIC detects tidal flats using brightness data from the satellite images, highly turbid water influences the brightness, and this may cause mis-detection of tidal flats in this area.

[Japan]

Japan has monitoring data on tidal flat distribution in the Seto Inland Sea and the Ariake Sea (Figure 4). These two sea areas are the main areas where tidal flats are distributed in Japan. Monitoring was conducted by the Ministry of the Environment, Japan to understand the current distribution in the Seto Inland Sea in 2015-2017 and in the Ariake Sea in 2019.

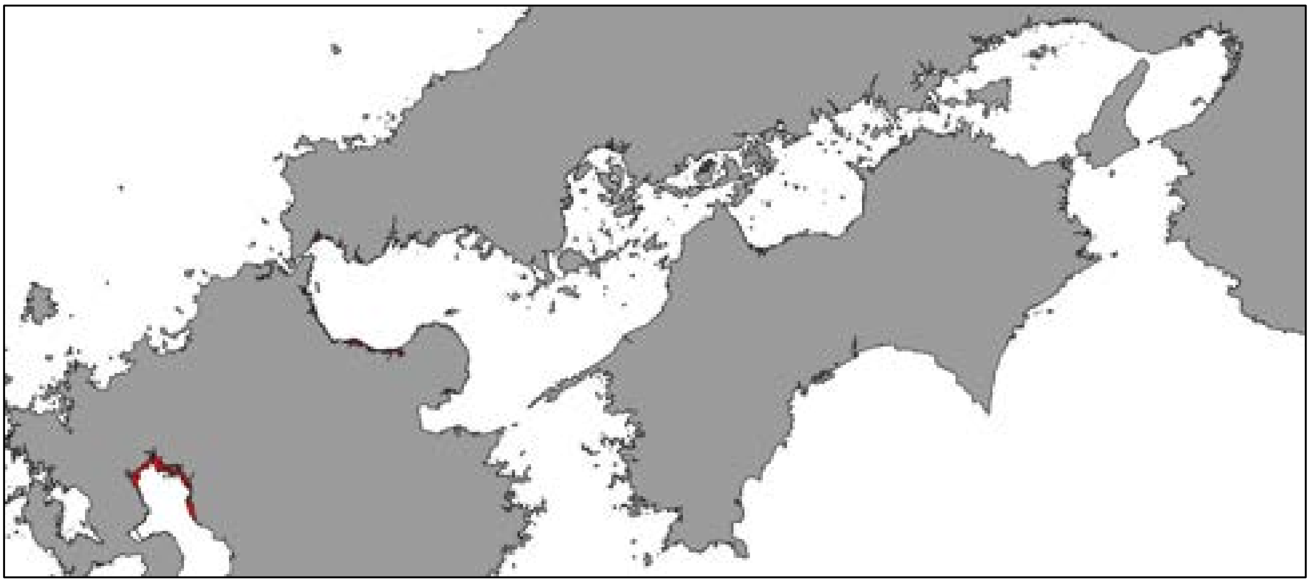

Figure 4. Tidal flat distribution in the Seto Inland Sea and the Ariake Sea.

The monitoring method is a combination of satellite image classification and in-situ surveys. Thirty-five RapidEye images (resolution of 5 m) between 2015-2017 are used for classification for the Seto Inland Sea and satellite images from Planet (resolution of 3 m) are used for the Ariake Sea. In both series of satellite images, sea areas between high-tide lines and low-tide lines are detected as tidal flat areas. The results of classification were validated using the real location from in-situ surveys.

The methodology is different between GIC and Japanese national monitoring, and it is shown that there is a substantial difference in detection of tidal flats in the two maps (Figure 5). A summary of error assessments is shown in Table 5.

Table 5. Comparison of the total area of tidal flats between national monitoring data and GIC data in Japan.

Sea area	*Area (ha)*			*Overlapped ratio (%)*
	National data	GIC	Overlapped	
Seto Inland Sea	11,066	3,912	1,929	17.4
Ariake Sea	18,738.9	4,806.1	4,216.0	22.5

Table 6. Detailed information on differences in national monitoring data (ND) and GIC detection of tidal flats in the Ariake Sea.

	National Data	GIC
Number of meshes	584	417
Total Area (ha)	18,739	4,806
Number of overlapped meshes	48	
Total overlapped area (ha)	4,216	
Overlapped ratio (%) (Overlapped area/Total area of ND)	22.5	
Overlapped ratio (%) (Num. of overlapped meshes/meshes of ND)	8.2	
Mis-detection ratio (%) (Un-overlapped area/Total area of ND)	12.3	

Table 7. Detailed information on differences in national monitoring data (ND) and GIC detection of tidal flats in the Seto Inland Sea.

	National Data	GIC
Number of meshes	822	1,017
Total Area (ha)	11,066	3,912
Number of overlapped meshes	58	
Total overlapped area (ha)	1,929	
Overlapped ratio (%) (Overlapped area/Total area of ND)	17.4	
Overlapped ratio (%) (Num. of overlapped meshes/meshes of ND)	7.1	
Mis-detection ratio (%) (Un-overlapped area/Total area of ND)	50.7	

Figure 5. Example of mis-detection of tidal flats in the Ariake Sea.

Pink areas indicate distribution of real tidal flats in the national provided data, and red areas indicate the distribution detected by GIC, with yellow areas as GIC's mis-detected areas.

As shown in Table 6 and 7 above, GIC accuracy is low in Japan. Mis-detection occurred in many areas and the size of detected tidal flats is underestimated. In GIC, riversides and water pools in landfill areas are mis-detected as tidal flats. In addition, due to the resolution of satellite images, small-size tidal flats under 10 ha cannot be detected.

Through additional analysis on the usefulness of GIC in Japan, one important point was identified. GIC uses Landsat satellite images for classification of tidal flats. Landsat is an earth observation satellite which has a polar, sun-synchronous orbit, and it passes at a fixed time on its trajectory. In case of Japan, the transit time of Landsat is 10:00-11:00 a.m. Figure 6 shows the relationship between the tide level change in the Ariake Sea and the transit time of Landsat over the Kyushu area in January of 2014. During the spring tide time, Landsat passes over the Kyushu area at high tide. On the other hand, during the neap tide time, Landsat passes at low tide. In either case, Landsat cannot take a snapshot of the maximum size of the tidal flat areas because of its transit time. Therefore, the area of tidal flats could be underestimated in Japan. This situation is same in China and Korea; thus underestimation is a common issue in the northwest Pacific region. Murray et al. (2019) also reported this problem and limitation as "the sun-synchronous orbit of Landsat satellites and sparse acquisition schedule (every 16 days) can lead to under-sampling of the full extent of tidal flats in the Landsat archive and, therefore, classification in the tidal flat map should be considered as 'observed tidal flat extent.'" GIC currently uses only Landsat satellite images; therefore, it is difficult to solve this problem soon. If other satellite image sources such as Sentinel and geostationary satellites are available for classification with GIC in the future, it will be able to calculate the real size of tidal flat areas in the northwest Pacific region.

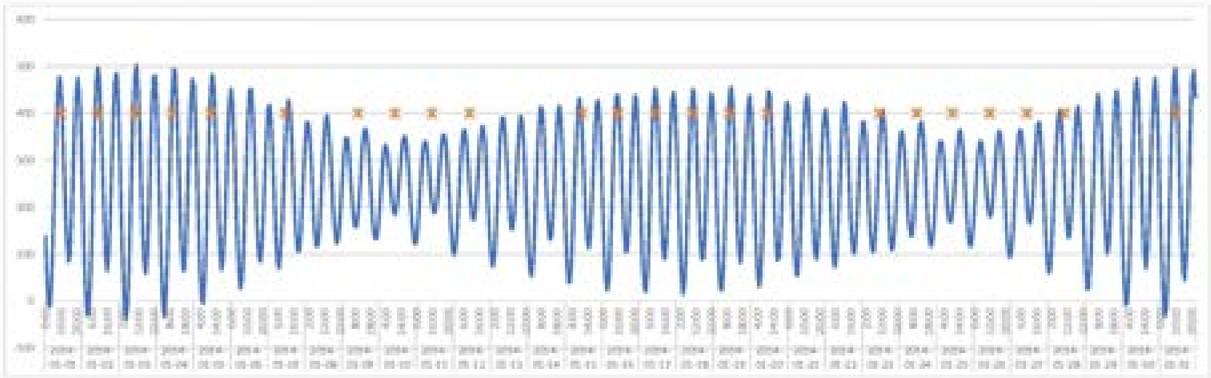

Figure 6. Tide level changes in the Ariake Sea in January 2014.

The blue line shows the tide level and yellow asterisks show the transit time of Landsat, used for classification in GIC.

Other detailed assessment results for the Seto Inland Sea are shown in the Annex.

[Korea]

Korea conducted in-situ surveys of tidal flats in the coastal areas in 2013. The distribution of tidal flats in Korea is shown in Figure 7. The main areas where tidal flats are distributed are the west and south coast of Korea. Also, the west coast of Korea faces the Yellow Sea and there are many tidal flats in this region.

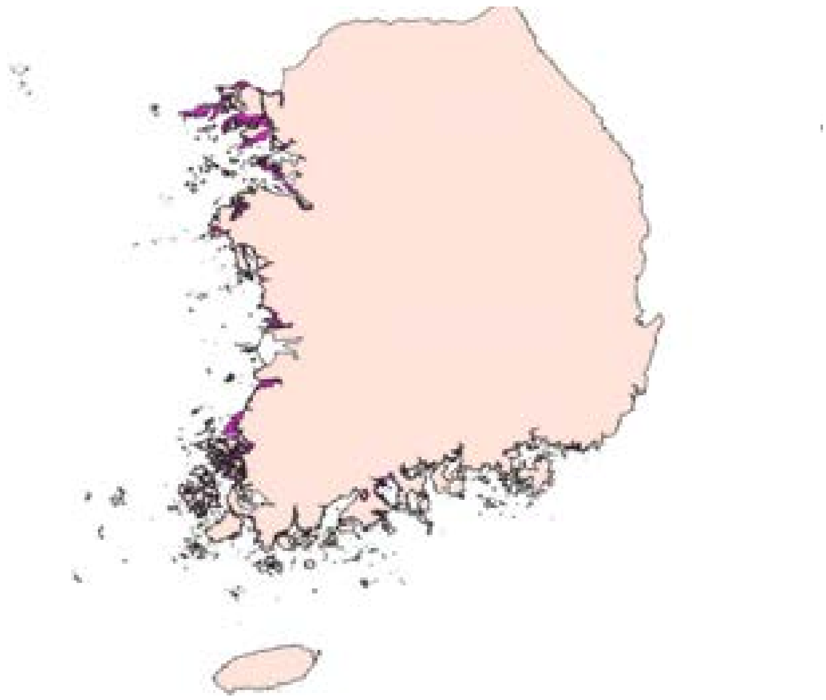

Figure 7. Distribution of tidal flats in Korea

Figure 8 shows the differences in GIC-distribution and the real distribution of tidal flats in the northwestern part of Korea (around Incheon and the estuary area of the Han River). As shown in the picture, most of the tidal flats detected by GIC and the real distribution overlap. However, as is the case in Japan, GIC areas are shown to underestimate the actual area when compared with the real distribution.

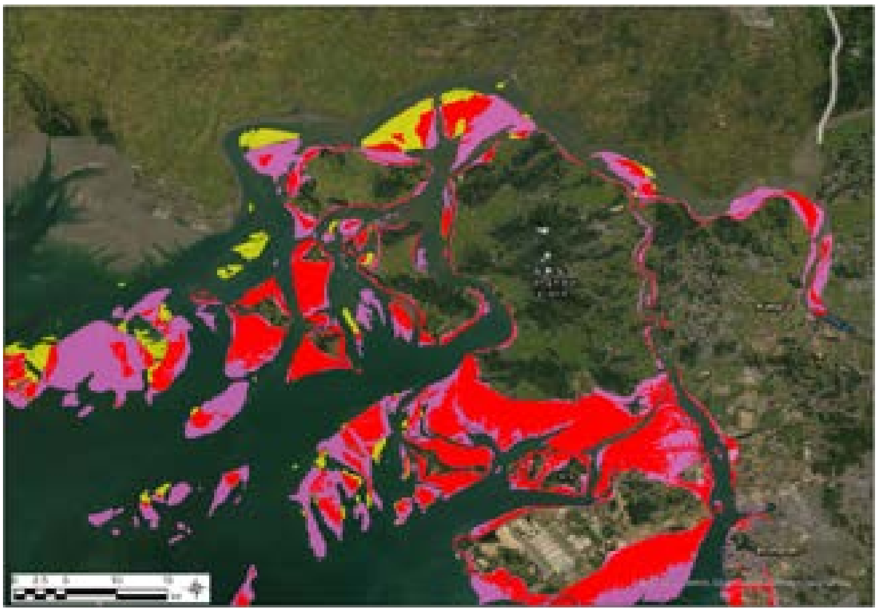

Figure 8. Distribution of tidal flats in the northeastern part of Korea
(around Incheon and the Han River estuary).

Pink areas indicate the real distribution of tidal flats provided from a Korean expert. Red areas are overlapped areas (national data and GIC), and yellow areas are areas mis-detected by GIC.

A summary of the assessment of differences in GIC distribution and the real distribution is shown in Table 8 and 9. GIC can detect the distribution of tidal flats with overlapped ratio of 56.2%. However, there are mismatches on quantitative information (total area of tidal flats). Differences such as this are expected to be resolved with improvements in GIC.

Table 8. Comparison of the total area of tidal flats between national monitoring data and GIC data.

Sea area	Area (ha)			Overlapped ratio (%)
	National data	GIC	Overlapped	
Eastern and southern coast of Korea	251,548.1	181,201.3	141,458.1	56.2

Table 9. Detailed information on differences in national monitoring data (ND) and GIC detection of tidal flats in Korea.

	National Data	GIC
Number of meshes	3,743	13,177
Total Area (ha)	251,548	181,201
Number of overlapped meshes	916	
Total overlapped area (ha)	141,458	
Overlapped ratio (%) (Overlapped area/Total area of ND)	56.2	
Overlapped ratio (%) (Num. of overlapped meshes/meshes of ND)	24.5	
Mis-detection ratio (%) (Un-overlapped area/Total area of ND)	21.9	

[Russia]

In Russia, tidal flats are distributed through the northern part of the NOWPAP region, around the Tatar Strait and coastal area of Sakhalin. Information available on the distribution of tidal flats in Russia was very limited; therefore, the accuracy of GIC is quite low compared with the other three countries. Figure 9 shows the differences in the distribution of tidal flats detected by GIC and the provided national data, and Table 10 and 11 show a comparison of the national data and GIC data.

Figure 9. Distribution of tidal flats in the northern part of Russia (around the Tatar Strait).
Pink areas indicate the real distribution of tidal flats provided from a Russian expert. Red areas show overlapped areas (national data and GIC), and yellow areas are areas mis-detected by GIC.

Table 10. Comparison of the total area of tidal flats between national monitoring data and GIC data.

Sea area	Area (ha)			Overlapped ratio (%)
	National data	GIC	Overlapped	
Coastal area of Sakhalin	2,640	4,176	1.2	0.05

Table 11. Detailed information on differences in national monitoring data (ND) and GIC data in Sakhalin, Russia.

	National Data	GIC
Number of meshes	3,260	1,540
Total Area (ha)	2,640	4,176
Number of overlapped meshes	4	
Total overlapped area (ha)	1.2	
Overlapped ratio (%) (Overlapped area/Total area of ND)	0.05	
Overlapped ratio (%) (Num. of overlapped meshes/meshes of ND)	0.1	
Mis-detection ratio (%) (Un-overlapped area/Total area of ND)	99.97	

3. Distribution maps of tidal flats/salt marshes in the NOWPAP region

Using the provided data (real distribution of tidal flats in NOWPAP member states) as new training data, GIC was improved by Dr. Nicholas Murray, and the first draft map was developed in June 2021. The distribution map of tidal flats in the NOWPAP region was improved from the original GIC mapping. However, there were still mis-detections in reclaimed areas and river mouths. Therefore, the CEARAC Secretariat asked experts from the member states to review the first draft map and remove/correct the obviously mis-detected tidal flats using a Google Earth application developed by Dr. Murray.

After review by the experts, the revised distribution map in the NOWPAP region was finalized and released at https://murrnick.users.earthengine.app/view/nowpap-app (Figure 10). The map shows the distribution of tidal flats every three years in the NOWPAP region and historical changes after 1986. The following pictures (Figure 11) show examples of distribution in major areas in NOWPAP member states detected using the improved GIC.

In 2017-2019 (the latest year of this mapping), a total of 740,776.5 ha of tidal flats were shown distributed in the NOWPAP region.

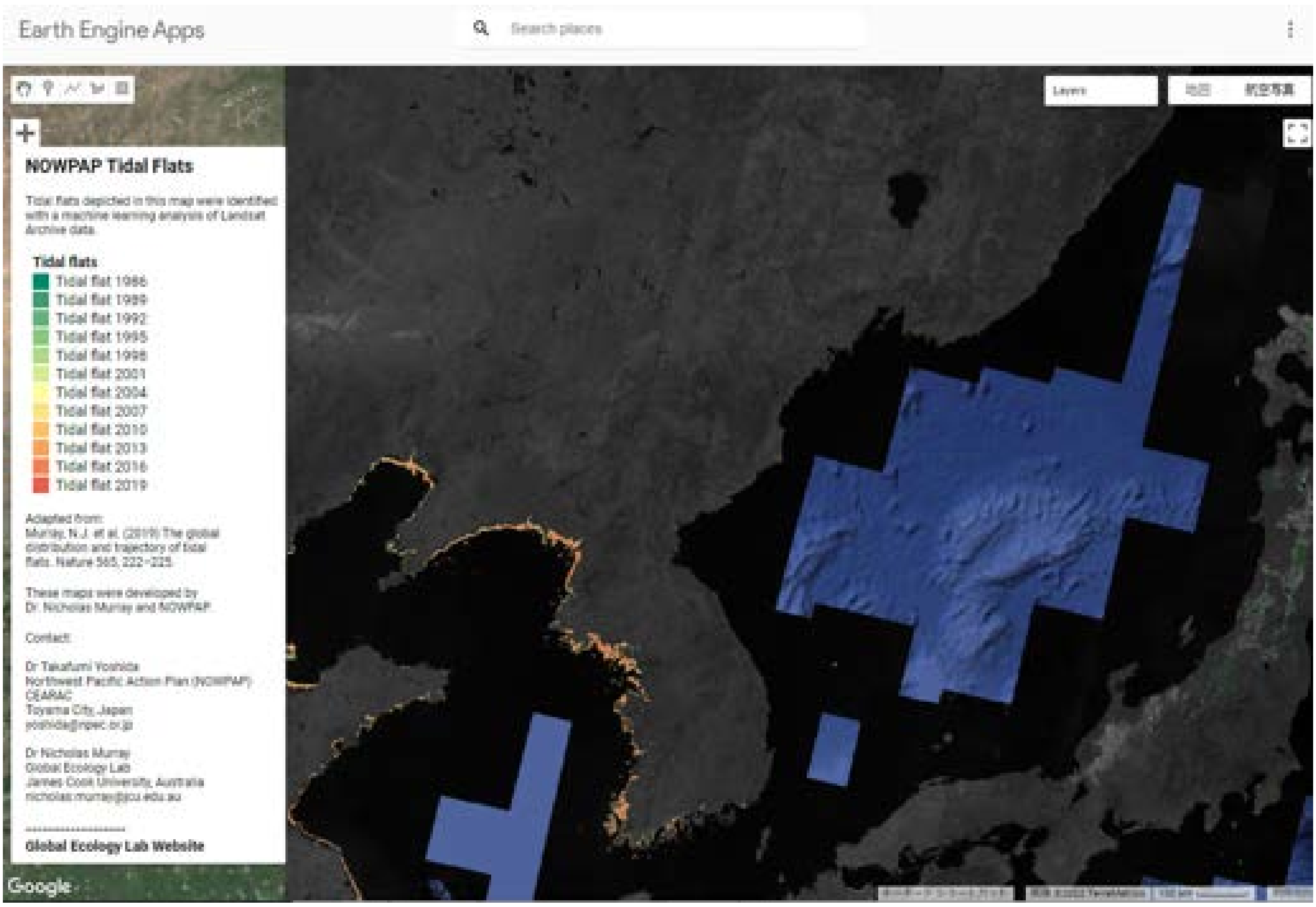

Figure 10. Tidal flat distribution in the NOWPAP region
(https://murrnick.users.earthengine.app/view/nowpap-app)

(a)

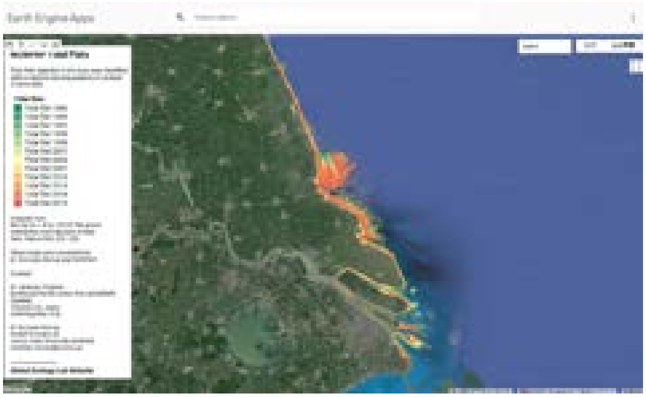

(b)

(c)

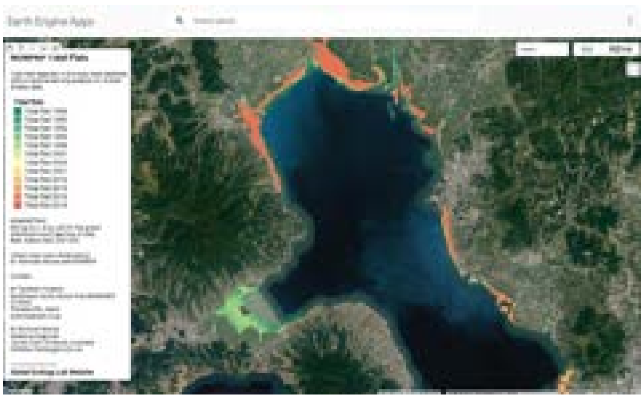

(d)

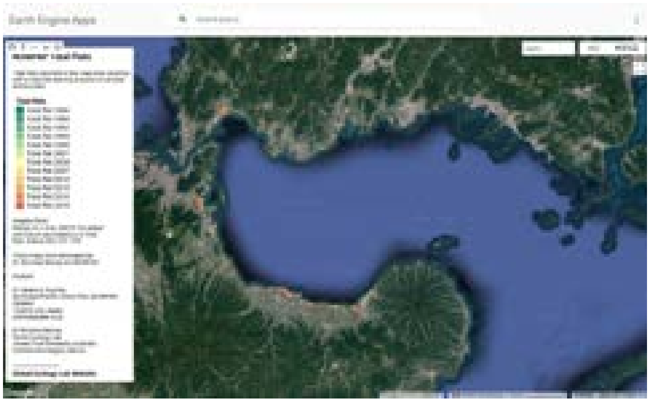

(e)

(f)

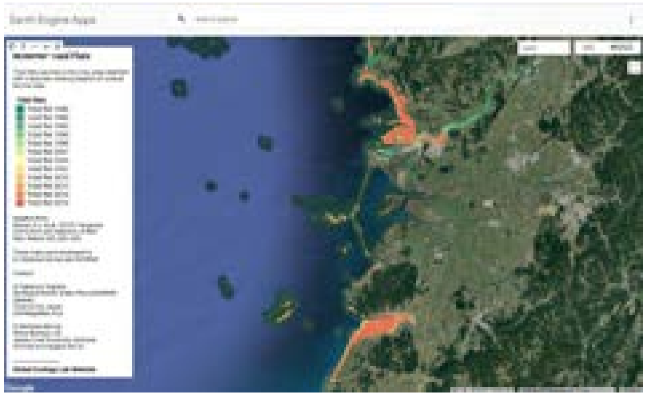

(g)

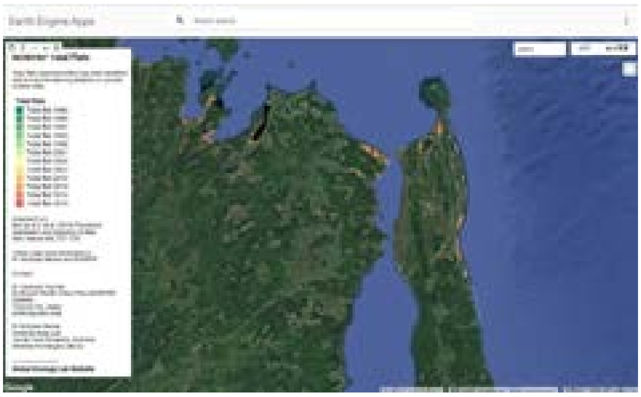

(h)

Figure 11. Distribution of tidal flats in major sea areas of NOWPAP member states.
(a) coastal area of the Changjiang River mouth, China, (b) coastal area of Shandong Peninsula, China, (c) Ariake Sea, Japan, (d) western part of the Seto Inland Sea, Japan, (e) offshore area of Incheon City, Korea, (f) Saemangeum, Korea, (g) Tatar Strait, Russia, (h) south Sakhalin, Russia.

3.1 Improvement of GIC for the NOWPAP region

By using national provided data as new training data, mis-detection of tidal flats was removed and the original GIC was improved, now being able to provide a more highly accurate distribution map in the NOWPAP region. There are still some difficulties and limitations in mapping the entire tidal flat distribution in the region. The following shows differences in tidal flat detection between the original GIC and the revised GIC, and improvement ratios in each NOWPAP member state.

[China]

In China, the revised GIC can prove higher accuracy in detection of distribution of tidal flats compared with the original tool (Figure 12). The revised GIC can detect tidal flat areas to almost the exact same degree as the national provided data. In addition, in the revised version, mis-detection in riversides and land areas (aquaculture ponds) was not found. The revised GIC was thusly improved in its detection ability.

However, several difficulties and limitations still remained (Figure 13, Table 12, 13). In the Yellow River estuary, there is a large gap in the number of tidal flats (mesh) between the provided national data and GIC data. While the provided data shows five tidal flat areas in this region, the revised GIC detects many tidal flat areas. The number of tidal flat areas was improved from the original and close to the national provided data, but a considerable gap remained. In addition to the gap in the number of tidal flats, the overlapped ratio of tidal flats between the GIC data and the national provided data is still low. As the Yellow River is famous for its highly turbid water, it may be difficult for GIC to detect tidal flats there.

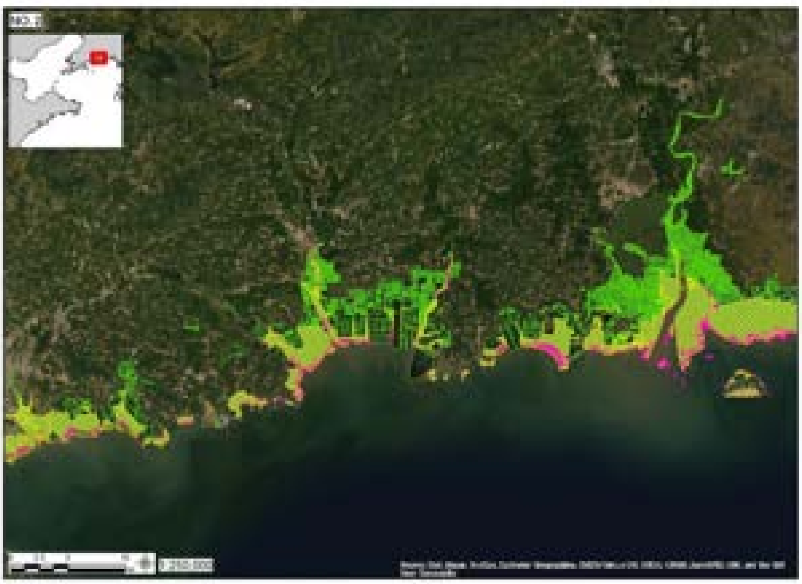

Figure 12. Differences in tidal flat distribution in the revised GIC, the original GIC, and the national provided data.
Pink areas show the real distribution (national provided data), yellow hatching areas are detected by the revised GIC, and green areas are detected by the original GIC.

Figure 13. Differences in tidal flat distribution in the revised GIC, the original GIC and the national provided data in the estuary of Yellow River.

Pink areas show real distribution (national provided data), yellow hatching areas are detected by the revised GIC, and green areas are detected by the original GIC.

Table 12. Differences in the national data (ND), the original GIC data, and the revised GIC data, and improvement in detection of tidal flats in the north area of the Yellow Sea, China.

	National Data	GIC (Original)	GIC (Revised)	Improvement ratio
Number of meshes	185	7,561	1,041	
Total Area (ha)	27,484	45,752	27,399	
Number of overlapped meshes with national data		146	95	
Total overlapped area (ha)		22,384	23,225	
Overlapped ratio (%) (Overlapped area/Total area of ND)		81.4	84.5	+3.8%
Overlapped ratio (%) (Num. of overlapped meshes/meshes of ND)		78.9	51.4	- 34.9%
Mis-detection ratio (%) (Un-overlapped area/Total area of ND)		51.1	15.2	+ 70.3%

Table 13. Differences in the national data (ND), the original GIC data, and the revised GIC, and improvement in detection of tidal flats in the Yellow River estuary, China.

	National Data	GIC (Original)	GIC (Revised)	Improvement ratio
Number of meshes	5	3,558	1,449	
Total Area (ha)	53,914	40,351	20,091	
Number of overlapped meshes with national data		5	5	
Total overlapped area (ha)		18,242	16,301	
Overlapped ratio (%) (Overlapped area/Total area of ND)		33.8	30.2	- 10.7%
Overlapped ratio (%) (Num. of overlapped meshes/meshes of ND)		100	100	
Mis-detection ratio (%) (Un-overlapped area/Total area of ND)		54.8	18.9	+ 65.5%

[Japan]

Differences in tidal flat distribution in the revised GIC data, the original GIC data, and the national provided data are shown in Figure 14. In Japan, the revised GIC has underperformed in detection of tidal flat distribution (Table 14, 15). The original tool showed a strong trend toward underestimating tidal flat areas, and this trend was not improved in the revised version. Mis-detections were removed dramatically, similar to detection in China; however, the overlapped ratio was not improved very much.

As reported in Chapter 2, one of the reasons for underestimation is the limitation of available Landsat satellite images. Most satellite images used in the GIC classification algorithm are taken at high tide or neap tide in Japan. This means that Landsat satellite images cannot show the full areas of tidal flats in Japan. If high-quality training data were provided, the classification algorithm could reflect such training data. Regarding this problem, it is expected that GIC will be able to use other satellite images at low tide or spring tide in the near future.

At present, even though the revised GIC has several limitations, it is a useful tool to identify locations of tidal flat areas in Japan, and the tool has the potential to map the distribution in this region.

Figure 14. Differences in tidal flat distribution in the revised GIC data (yellow hatching areas), the original GIC data (green areas), and the provided national data (pink areas) in the western part of the Seto Inland Sea.

Table 14. Differences in the national data (ND), the original GIC data, and the revised GIC, and improvement in detection of tidal flats in the Ariake Sea, Japan.

	National Data	GIC (Original)	GIC (Revised)	Improvement ratio
Number of meshes	584	417	181	
Total Area (ha)	18,739	4,806	4,539	
Number of overlapped meshes with national data		48	22	
Total overlapped area (ha)		4,216	4,410	
Overlapped ratio (%) (Overlapped area/Total area of ND)		22.5	23.5	+ 4.4%
Overlapped ratio (%) (Num. of overlapped meshes/meshes of ND)		8.2	3.8	- 53.7%
Mis-detection ratio (%) (Un-overlapped area/Total area of ND)		12.3	2.9	+ 76.4%

Table 15. Differences in the national data (ND), the original GIC data, and the revised GIC data, and improvement in detection of tidal flats in the Seto Inland Sea, Japan.

	National Data	GIC (Original)	GIC (Revised)	Improvement ratio
Number of meshes	822	1,017	108	
Total Area (ha)	11,066	3,912	1,900	
Number of overlapped meshes with national data		58	24	
Total overlapped area (ha)		1,929	1,724	
Overlapped ratio (%) (Overlapped area/Total area of ND)		17.4	15.6	- 10.3%
Overlapped ratio (%) (Num. of overlapped meshes/meshes of ND)		7.1	2.9	- 59.2%
Mis-detection ratio (%) (Un-overlapped area/Total area of ND)		50.7	9.3	+ 81.7%

[Korea]

In Korea, the revised GIC has the same predisposition as China and Japan, and mis-detection of tidal flats was removed from the original version. The revised GIC shows the locations of tidal flats in Korea with a high degree of accuracy; however, quantitative information shows poor performance (underestimation) (Table 16).

As shown in Figure 15, due to past reclamation projects (Saemangeum Seawall Project), a huge tidal flat was lost. This change was shown more accurately in the revised GIC data.

Figure 15. Differences in tidal flat distribution in the revised GIC data (yellow hatching areas), the original GIC data (green areas), and the national provided data (pink areas) in the coastal area of Saemangeum in Korea.

Table 16. Differences in the national data (ND), the original GIC data, and the revised GIC data, and improvement in detection of tidal flats in the west and south coast of Korea.

	National Data	GIC (Original)	GIC (Revised)	Improvement ratio
Number of meshes	3,743	13,177	3,867	
Total Area (ha)	251,548	181,201	153,726	
Number of overlapped meshes with national data		916	504	
Total overlapped area (ha)		141,458	142,796	
Overlapped ratio (%) (Overlapped area/Total area of ND)		56.2	56.8	+ 1.1%
Overlapped ratio (%) (Num. of overlapped meshes/meshes of ND)		24.5	13.5	- 44.9%
Mis-detection ratio (%) (Un-overlapped area/Total area of ND)		21.9	7.1	+ 67.6%

[Russia]

The original GIC data showed very large gaps in comparison with the provided national data and quite low performance in detection of tidal flats in the coastal area of Russia. By adding the provided national data as training data, this low performance was improved dramatically (Figure 16 and Table 17). However, the national data is not enough for quantitative discussion of tidal flats in Russian coastal waters. More information on real distribution is expected to be accumulated in the future, along with an increase in available satellite images in the future.

Figure 16. Differences in tidal flat distribution in the revised GIC data (yellow hatching areas), the original GIC data (green areas), and the national provided data (pink areas) in Sakhalin, Russia

Table 17. Differences in the national data (ND), the original GIC data, and the revised GIC data, and improvement in detection of tidal flats in Sakhalin, Russia.

	National Data	GIC (Original)	GIC (Revised)	Improvement ratio
Number of meshes	3,260	1,540	546	
Total Area (ha)	2,640	4,176	5.006	
Number of overlapped meshes with national data		4	74	
Total overlapped area (ha)		1.2	436	
Overlapped ratio (%) (Overlapped area/Total area of ND)		0.05	16.5	+ 33,000%
Overlapped ratio (%) (Num. of overlapped meshes/meshes of ND)		0.1	2.3	+ 2,300%
Mis-detection ratio (%) (Un-overlapped area/Total area of ND)		99.97	91.3	+ 8.7%

3.2 General conclusion regarding the revised GIC

The revised GIC was improved from the original version in the detection of tidal flat distribution, and it can provide a more useful distribution map in the NOWPAP region. One major improved point is the decrease of mis-detection. In the original tool, many instances of mis-detection occurred in coastal areas and land areas. Riversides in downstream basins were detected as tidal flat areas in many NOWPAP member states. In China, aquaculture is very active and many aquaculture ponds are developed along the coast. These ponds were classified as tidal flats by the original GIC. These mis-detections were almost completely removed in the revised GIC. It is difficult to remove mis-detection completely, however, and several mis-detections remained (Table 18). Through these improvements, the revised GIC can detect the distribution of tidal flats with higher accuracy in the NOWPAP region. There are still considerable gaps in Russia, however, because of the limitation of available information on real distribution and lack of available satellite images. It is expected that the revised GIC will provide highly accurate information in the future through the inclusion of additional information and training data in Russia.

The revised GIC has several difficulties in understanding the quantitative information on tidal flats in the NOWPAP region. The revised version still tends to underestimate tidal flat areas in the region. One of the reasons is the satellite images that are used for classification. Due to the limitation of use of appropriate satellite images at different tidal levels, GIC has difficulties in estimating the full areas of tidal flats. Therefore, in China, Japan, and Korea, the total area of tidal flats was underestimated. Another reason is the highly turbid water in the Yellow Sea. High turbidity prevents GIC from detecting tidal flats in the Yellow Sea. Both difficulties may be solved by using additional satellite sensors other than Landsat and developing a classification algorithm. In the near future, a more suitable mapping tool for the NOWPAP region to understand quantitative information will then be developed.

Table 18. Mis-detection of the revised GIC in NOWPAP member states.

Country	Sea-area	Sub-area	Number of mis-detection	Area of mis-detection (ha)
China	North Yellow Sea	Islands	20	116.0
		Coastal area	50	171.5
		Land	84	252.6
		River	120	336.3
	Estuary of the Yellow Sea	Land	283	937.4
		River	134	360.2
Japan	Ariake Sea	Coastal area	3	0.4
		River	4	0.9
	Seto Inland Sea	Coastal area	2	28.2
		Land	3	23.3
		River	4	66.2
Korea	Western and southern coast	Islands	16	165.6
		Coastal area	29	263.2
		Inner bay	45	205.5
		Landfill	40	166.1
		River	35	229.6
Russia	Coast of Sakhalin	Coastal area	483	3858.5
		Inner bay	9	150.5
Total			1,364	7,332

3.3 Good Practice with the revised GIC

Figure 17 shows one of the good mapping practices using the improved GIC. Tokyo Bay is located out of the NOWPAP region. It is, however, one of the most developed enclosed seas in Japan. In the past, there were many tidal flats visible in this area, but because of rapid coastal development, many of the tidal flats were lost. At present, a few valuable tidal flats remain in the bay. Yazu tidal flat is one of these, and local citizens and government protect it as a Ramsar Convention site. Small-size tidal flats like these can be detected by the improved GIC, if good training data are available in a target area. NOWPAP member states are trying to restore their tidal flats, and the improved GIC may be used to monitor restoration of the tidal flats.

Figure 17. Distribution of tidal flats in Tokyo Bay in 2005-2007.
A is Yazu Tidal Flat and B is Sanbanze Tidal Flat, which are valuable tidal flats near the metropolis.

4. Historical changes in tidal flat distribution and contributing factors

Murray et al. (2014) estimated that the loss of tidal flats from the 1950s to 2000s in the Chinese coastal area of the Yellow Sea and the Bohai Sea is 378,728 ha, and 229,859 ha in the Yellow Sea of Korea, respectively. During the past four decades, about 70% of total tidal flats in the Yellow Sea were lost.

The Northwest Pacific region is one of the most populated regions with economic growth in the world. To shore up such a rapid population concentration and economic development, NOWPAP member states have a long history of coastal development (NOWPAP DINRAC 2021). In China, recent active reclamation started in the 1950s. By the end of the last century, a total of 1.2 million hectares were reclaimed. There were four main waves of coastal development, the first being sea reclamation in the 1950s for developing salt fields, the second being reclamation in the mid-1960s to 1970s for developing agricultural land, the third in the 1980s and 1990s for developing aquaculture ponds, and the last being recent reclamation for constructing industrial and economic zones due to rapid economic growth. In 2015, a total of 11,055.29 hectares of sea area were reclaimed.

In Japan, a boom of reclamation happened in the 1970s, and the maximum 55 km^2 of sea area was reclaimed in 1975. Reclamation then decreased due to the regulation of coastal development, and recent reclamation has been less than 5 km^2 per year. Main target areas of sea reclamation are not in the NOWPAP region but on the Pacific side, on the south coast of Japan around metropolitan areas such as Tokyo, Nagoya, and Osaka. Due to sea reclamation, 3,857 ha of tidal flats, 7% of the total tidal flat area in Japan, were lost from 1978 to 1988 (MoE, 1994).

Reclamation activities in Korea can be divided into two phases: before and after 1991, when the national reclamation master plan was established. In the 1960s and 70s, sea areas were reclaimed for agricultural land. In the late 1980s, large-scale reclamation started, and after 1991, huge reclamation projects started, including the Shiwa District Development Project and Saemangeum reclamation project.

Yim et al (2018) reported on the historical reclamations in the coastal areas of China and Korea in the Yellow Sea (Table 19). As shown in Table 19, a total of approximately 9,000 km^2 of sea area was reclaimed over the past forty years. This reclamation had a strong impact on reduction of tidal flat areas in the Yellow Sea.

In Russia, large-scale reclamation projects were not reported.

GIC mapping can show historical changes in tidal flats in NOWPAP member states after 1986. Two examples are introduced as follows:

In the Ariake Sea, Japan, a huge tidal flat area was lost due to land reclamation in 1997. Isahaya Bay was originally an enclosed bay that had a huge tidal flat. To create agricultural land, the bay was closed in 1997. In Figure 18, a huge tidal flat was seen in 1997; however, it has been lost in the picture from 2019.

Table 19. Historical reclamation changes in the Yellow Sea.
(modified based on Yim et al., 2018)

	Area of coastal reclamation (km^2)				
	1980s	1990s	2000s	2010s	Total
China					7367
Liaoning	573	235	656	253	1717
Hebei	170	86	431	150	837
Tianjin	19	17	272	92	400
Shandong	1284	231	797	345	2657
Jiangsu	315	609	567	265	1756
Korea					1580
Incheon	-	46	-	-	46
Gyeonggi	-	211	62	-	273
Chungnam	230	56	14	-	390
Jeonbuk	-	-	401	-	461
Jeonnam	138	226	46	-	410

Figure 18. Comparison of tidal flat distribution between 1995 and 2019 in Isahaya Bay, Japan. Green areas show the distribution in 1995, and red areas show distribution in 2016.

Figure 19 is another example of the loss of tidal flats in the NOWPAP region due to past coastal developments. Figure 19 shows the distributions of tidal flats in 1986 and 2019 in the coastal area of Incheon, Korea. Green colors indicate the distribution in 1986 and red colors are from 2016. Before the Incheon International airport opened in 2001, construction work for the airport and land reclamation started in 1992. In 1986, the sea area where the airport is now located was tidal flats, and GIC is able to identify the past distribution.

Figure 19. Historical tidal flat distribution changes in Korea.

The red arrow in the picture shows the loss of tidal flats due to the construction of the Incheon International Airport.

Figure 20 shows historical changes in the total tidal flat area in the NOWPAP region. It is very difficult to show an accurate quantitative change because of the availability of satellite images for each year. GIC, however, shows a decreasing trend in the NOWPAP region.

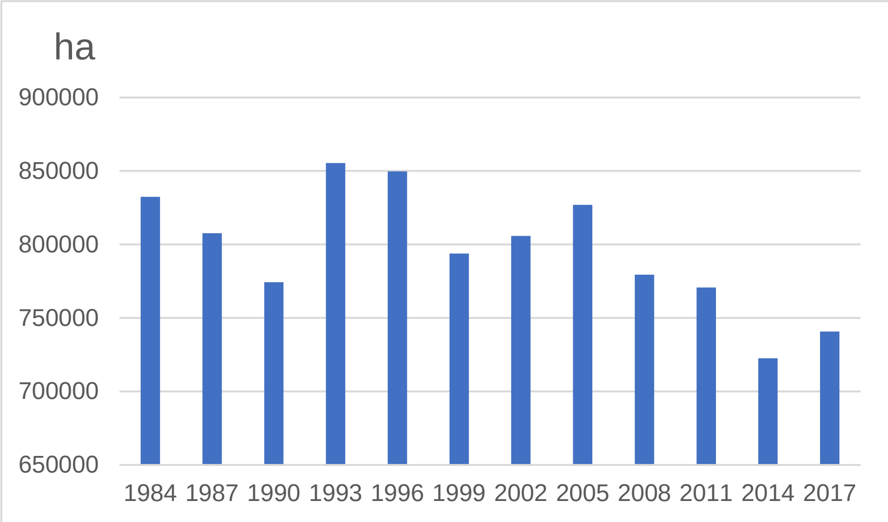

Figure 20. Historical changes in tidal flat areas in the NOWPAP region from the 1980s.

5. Summary

A tidal flat is one of the significant coastal habitats for marine biodiversity conservation in the NOWPAP region. Mapping tidal flats is the first step for conservation of these habitats. The improved Global Intertidal Change (GIC) mapping tool can provide useful information on the geographical tidal flat locations in this region, and the activities being conducted to map tidal flat distribution in the NOWPAP region can help advance tidal flat conservation.

Both the benefits and limitations/difficulties of tidal flat mapping using satellite images have been identified through these activities. While the improved GIC produced a highly accurate distribution map compared with the original tool, underestimations and mis-detections still occur. There are several different reasons for these defects.

One reason is the limitation of available real distribution data (training data) for the NOWPAP region. Due to the technological development with clarification algorithms and the increase of available high quality satellite images, coastal habitat mapping using remote sensing techniques has become increasingly utilized in recent years. Therefore, in the near future, accumulation of case studies in the NOWPAP region will provide useful training data for mapping projects with remote sensing technology.

Another reason for shortcomings in the GIC is the quality of satellite images used in the classification of tidal flats. In GIC, satellite images from Landsat are used. Its resolution is 30 m, without enough detail to classify small-scale tidal flats. In China and Korea, wide tidal flats are distributed. However, in Japan, there are lots of small-scale tidal flats, of sizes smaller than 0.1 ha. With the current classification algorithm, it is difficult to classify such small sizes. In recent years, as more high-resolution satellite images are available for free, this problem will be solved soon.

The sizes of tidal flats detected by GIC are often underestimated compared to the actual flats. GIC uses machine learning (Random Forest Classification Algorithm), and the results are validated by machine learning using training data. On the other hand, Japanese monitoring detects tidal flats using satellite images of high and low tides. This method can produce quantitative data with high accuracy.

This method, however, requires more human power and time to select quality satellite images. Machine learning using a cloud computing platform is an advantageous characteristic of GIC that reduces the manual workload. In the future, it is expected that machine learning techniques will be increasingly developed and a more useful mapping tool will be introduced.

The Ministry of Ocean and Fisheries (MOF) in Korea firstly planned tidal flat restoration in 2008 and 17 target areas were selected. Over 20 million US dollars were spent for restoration in the selected areas (over 2 km^2) from 2010 to 2014 (Kwon and Khim, 2018). The MOF then developed "The Tidal Flat Resources Master Plan" in 2015 and "The Master Plan on Management and Ecological Restoration of Tidal Flat and Adjacent Areas, first edition (2021-2025)" in September 2021, as continued substantial efforts in the restoration of tidal flats. In addition to the second master plan, the Korean government established the Marine Protected Areas (MPA) Management Plan. Valuable tidal flats in Korea are selected as MPAs, and Korean government puts forth considerable effort toward the conservation and restoration of tidal flats.

In the other three countries, the restoration of altered tidal flats is promoted actively. China developed a new management system using Marine Ecological Red Lines (People's Republic of China Ministry of Environmental Protection (2015), Zhang et al. (2017), Yang et al. (2018)), and Japan promotes a healthy material cycle, high production, and biodiversity in coastal areas based on the Marine Healthy Plan and Sato-Umi (http://www.env.go.jp/water/heisa/satoumi/en/index_e.html). Detailed information on recovered tidal flats in the NOWPAP region has not been reported yet, so it is still unclear to what degree the effects of such restoration efforts are reflected in the historical change of the tidal flat areas. When focusing on specific areas where restoration activities are conducted, the improved GIC will be able to monitor positive changes in tidal flats in the NOWPAP region.

6. References

Chen Y., J. Dong, X. Xiao, Z. Ma, K. Tan, D. Melville, B. Li, H. Lu, J. Liu and F. Liu (2019): Effects of reclamation and natural changes on coastal wetlands bordering China's Yellow Sea from 1984 to 2015, Land Degradation and Development, https://doi.org/10.1002/ldr.3322

Choi J-K, J-H Ryu, Y-K Lee, H-R Yoo, H.J. Woo and C.H. Kim (2010): Quantitative estimation of intertidal sediment characteristics using remote sensing and GIS, Estuarine, Coastal and Shel Science, 88, 125-134

Kwon B-O and J.S. Khim (2018): Coastal Reclamation and Restoration in RO Korea, The 3rd YSLME Science Conference

Lee Y-K, J-H Ryu, J-K Choi, S. Lee and H-J Woo (2015): Satellite-based observations of unexpected coastal changes due to the Saemangeum Dyke construction, Korea, Marine Pollution Bulletin, 97, 150-15

MacKinnon J., Y.I. Verkuil and N. Murray (2012): IUCN situation analysis on East and Southeast Asian intertidal habitats, with particular reference to the Yellow Sea (including the Bohai Sea). Occasional Paper of the IUCN Species Survival Commission No. 47. IUCN, Gland, Switzerland and Cambridge, UK. ii + 70 pp.

Ministry of Environment, Japan (1980): The 2nd Natural Environment Research: Tidal Flats, Seaweed Beds and Coral Reefs Survey

Murray N.J., R.S. Clemens, S.R. Phinn, H.P. Possingham and R.A. Fuller (2014): Tracking the rapid loss of tidal wetlands in the Yellow Sea, Front. Ecol. Environ., doi:10.1890/13026

Murray N.J., S.R. Phinn, M. DeWitt, R. Ferrari, R. Johnston, M.B. Lyons, N. Clinton, D. Thau and R.A. Fuller (2019): The global distribution and trajectory of tidal flats, Nature, 565, doi: 10.1038/s41586-018-0805-8

NOWPAP DINRAC (2021): Report on Sea Reclamation State and Management in NOWPAP region

People's Republic of China Ministry of Environmental Protection (2015): Technical guide for ecological red line, No. 2015.5 (Chinese Ministry of Environmental Protection, Beijing, China, 2015)

Ryu J-H, J-K Choi and Y-K Lee (2014): Potential of remote sensing in management of tidal flats: A case study of thematic mapping in the Korean tidal flats, Ocean and Coastal Management, 102, 458-470

Ryu J-H and Y-K Lee (2018): Remote Sensing of Korean Tidal Flats, Remote Sensing of the Asian Seas, 221-235

Yang B., C.P. Wong, B. Jiang, A.C. Hughes, M. Wang and Q. Wang (2018), Developing China's Ecological Redline Policy using ecosystem services assessments for land use planning, nature communications, 9:3034, DOI: 10.1038/s41467-018-05306-1

Yang S-L. and J-Y. Chen (1995): Coastal salt marshes and mangrove swamps in China. Chinese Journal of Oceanology and Limnology, 13, 318-324

Yim J., B-O Kwon, J. Nam, J.H. Hwang, K. Choi and J.S. Khim (2018): Analysis of forty years long changes in coastal land use and land cover of the Yellow Sea: The gains or loss in ecosystem services, Environmental Pollution, 241, 74-84

Zhang K., X. Dong, Z. Liu, W. Gao, Z. Hu and G. Wu (2019): Mapping Tidal Flats with Landsat 8 Images and Google Earth Engine: A Case Study of the China's Eastern Coastal Zone circa 2015, Remote Sensing, 11, 924; doi:10.3390/rs11080924

Zhang Y, C. Chu, L. Liu, S. Xu, X. Ruan and M. Ju (2017): Water Environment Assessment as an Ecological Red Line Management Tool for Marine Wetland Protection, Int. J. Environ. Res. Public Health, 14, 870, doi: 10.3390/ijeeph14080870

7. Annex

Error assessment of Global Intertidal Change (GIC) in the Seto Inland Sea: Comparison between GIC data and real distribution data

Global Intertidal Change (GIC) is used for mapping the tidal flat distribution in the NOWPAP region. However, as explained in Chapter 2, there is a considerable difference between the tidal flat distribution detected by GIC and real distribution data supplied through national monitoring. Additionally, there are some technical limitations in GIC. The differences are caused by differences in the satellite images used, methodologies for tidal flat detection, and validation (Table A-1). To understand the differences in and limitations of GIC, detailed assessment was implemented in the case of the Seto Inland Sea.

Table A-1. Features of GIC and Monitoring in Japan

	Global Intertidal Change	Monitoring in Japan
Satellite	Landsat 4, 5, 7, 8	RapidEye
Sensor	Multiband	Multiband
Resolution	30 m	5 m
Validation	Online validation application in Google Earth Engine, Bootstrapping approach, post hoc sensitivity analysis	In situ survey
Number of used satellite images	707,528 images from 1984-2016 Within 1 km of the coastline	35 images from 2015-2017
Timing of satellite images	-	High tide and low tide
Methodology	Random-forest classification algorithm - Development of a globally distributed training dataset - Experienced analyst (N.J.M.) used high-spatial-resolution satellite imagery, global-scale bathymetry data, multiple Landsat-derived spectral reflectance variables and image time-series data from Google earth and Landsat - Three-year time period - Surface reflectance (FMask algorithm), Normalized Difference Water Index, Automated Water Extraction Index, Normalized Differenced Vegetation Index	Area surrounded by a high tide line and low tide line is identified as tidal flat. - High tide line is estimated from water extraction index. - Low tide line is estimated from water depth and brightness.

Maps (Figure A-1) show the differences in tidal flat distribution in GIC data and national monitoring data. In the Suo Nada Sea, the western part of the Seto Inland Sea, wide tidal flat areas are distributed. However, the sizes of the tidal flat areas detected by GIC are underestimated. One of the reasons of this underestimation is in differences in the applied methodology, in particular how tidal flat areas are detected, between GIC and Japanese national monitoring. Japanese monitoring detects tidal flat areas using satellite images (RapidEye) and information on high tide/low tide. It can therefore show a high-precision distribution map. On the other hand, GIC detects tidal flats using a random-forest classification algorithm and the obtained data are validated by training data. In the NOWPAP region, training data are quite limited; therefore, the accuracy of detection in GIC is lower than the real distribution.

In the eastern part of the Seto Inland Sea, the situation is different from the western part, and small-scale tidal flats are distributed in the estuary. Small-scale tidal flats like these are not detected by GIC, possibly due to the resolution of satellite images and/or limitation of available training data.

In addition, some mis-detection is identified in GIC. GIC classified ponds in landfill areas (offshore airports, etc.), estuaries, and riversides as tidal flats. This may be caused by limited available training data in the coastal area of Japan. Therefore, by adding provided national data on real distribution, the distribution data of tidal flats by GIC is expected to be improved.

Kii Strait

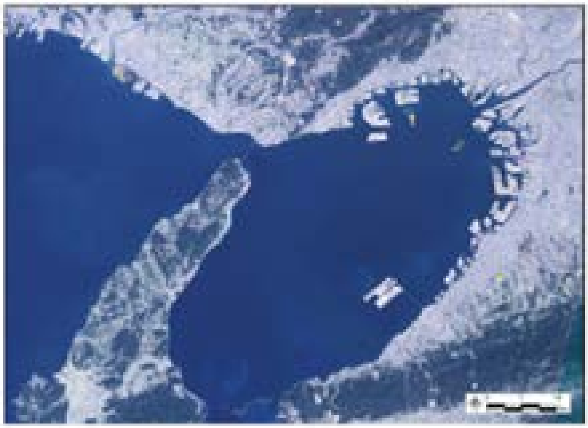

Osaka Bay

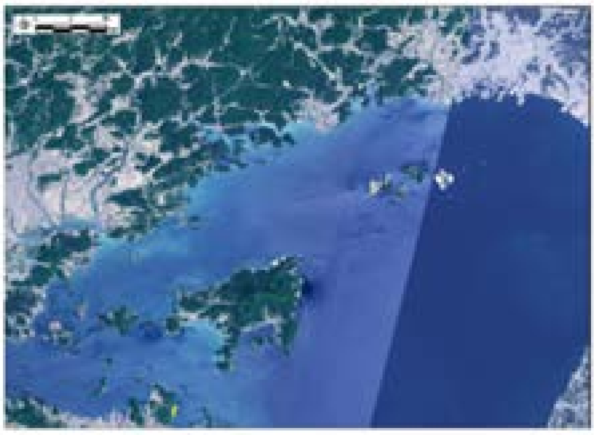

Harima Nada Sea

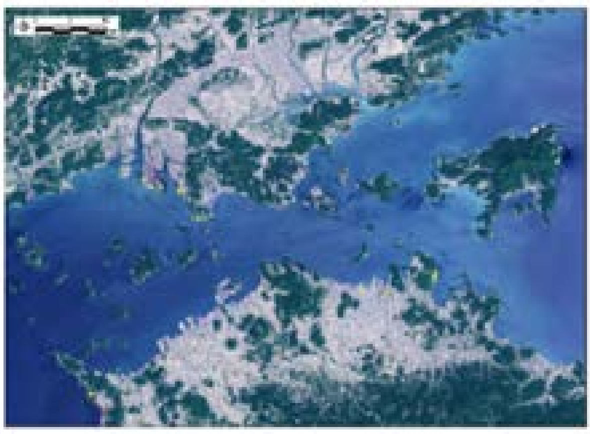

Bisan-Seto

Bingo Nada Sea

Hiuchi Nada Sea

Hiroshima Bay

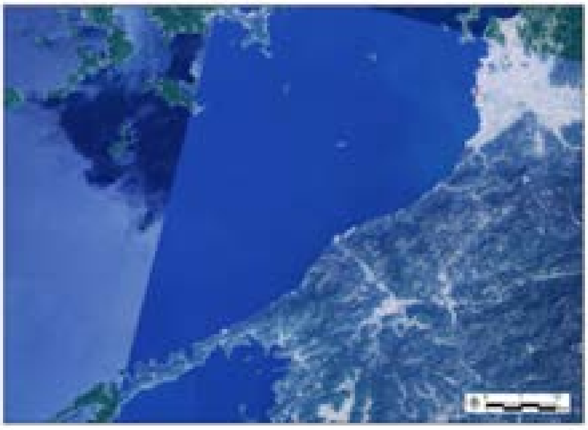

Iyo Nada Sea (east)

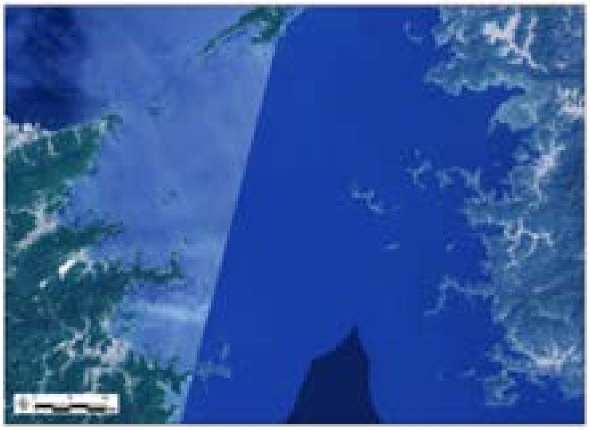

Bungo Strait

Iyo Nada Sea (west)

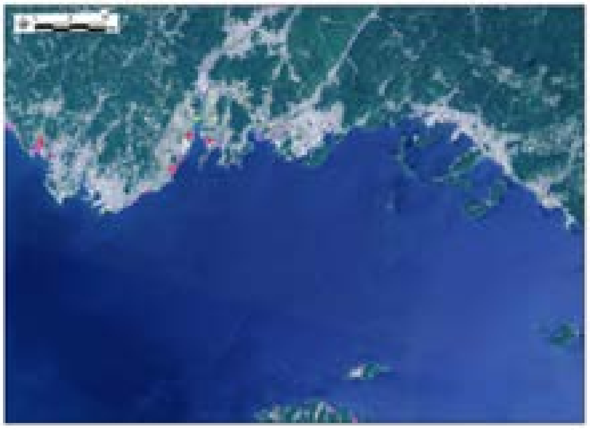

Suou Nada Sea

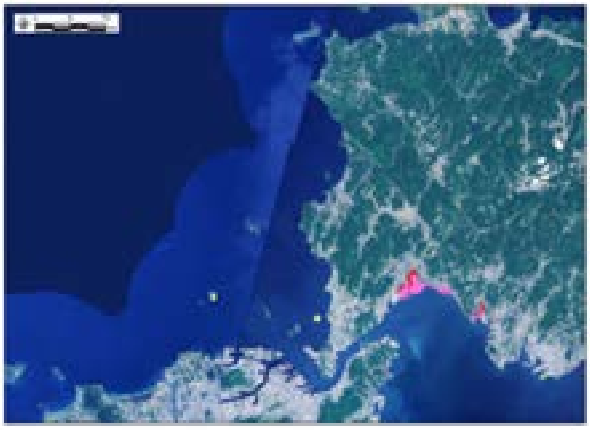

Hibiki Nada Sea

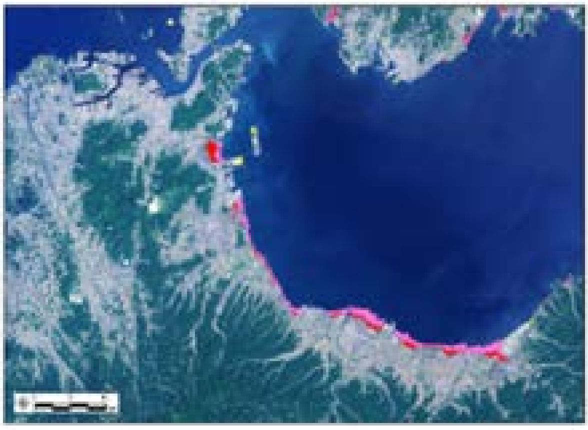

Suou Nada Sea

Figure A-1. Distribution of tidal flats in the Seto Inland Sea.
(Yellow parts indicate tidal flat areas identified by Global Intertidal Change (GIC), and pink areas are survey results from the Ministry of the Environment (MoE), Japan. Red areas are overlapped areas of the GIC and MoE surveys)

Table A-2 and A-3 show the total area (ha) of tidal flats in provided national data and GIC data in each sub-sea area in the Seto Inland Sea, and their overlapped rate. As shown in the table, GIC detected a great deal of tidal flats in the Seto Inland Sea. The locations of most tidal flats, however, are different from the real ones. Mismatching between the two data sets is quite high in all sub-sea areas. Wide tidal flats are distributed throughout the western part of the Seto Inland Sea, and the overlapped ratio is little higher than other sub-sea areas. This means that GIC has a weakness in identifying small-scale tidal flats. Table A-4 shows the number of tidal flats in each horizontal size, and wide tidal flats (over 50 ha) are detected with high accuracy compared with smaller flats. In the Yellow Sea, tidal flats are wider than those in the Japanese coastal area. Therefore, the accuracy of GIC detection in the Yellow Sea will be higher.

Table A-2. Differences in the areas detected as tidal flats by Japanese monitoring and GIC in each sub-sea area of the Seto Inland Sea, Japan

Sea area		Area (ha) Japan	Area (ha) GIC	Area (ha) Overlapped area	Overlapped ratio (%)
East	Kii Strait	203.5	53.7	9.3	4.6
	Harima Nada	367.2	192.9	3.4	0.9
	Osaka Bay	46.5	50.2	0.0	0.0
	Bisan-Seto	406.1	193.7	10.8	5.6
Center	Bingo Nada	338.7	187.1	42.3	2.7
	Hiuchi Nada	1,448.3	736.5	115.8	8.0
	Aki Nada	176.2	11.7	0.0	0.0
	Hiroshima Bay	838.1	45.2	8.6	1.0
	Iyo Nada	625.4	189.0	129.2	20.7
West	Bungo Strait	69.3	8.3	0.0	0.0
	Suou Nada	6,541.4	2,155.8	1,609.4	24.6
	Hibiki Nada	46.1	87.5	0.0	0.0
Total		11,106.7	3,911.6	1,928.8	

Table A-3. Number of tidal flats detected by MoE and GIC in each sub-sea area

Sea area		MoE	GIC	Num. of mismatch of GIC with MoE	Mismatching rate (mismatch/MoE)
East	Kii Strait	13	16	11	84.6
	Harima Nada	46	94	45	97.8
	Osaka Bay	6	40	6	100.0
	Bisan-Seto	48	131	46	87.0
Center	Bingo Nada	48	42	39	95.8
	Hiuchi Nada	182	174	172	94.5
	Aki Nada	42	6	42	100.0
	Hiroshima Bay	182	35	180	98.9
	Iyo Nada	105	38	99	60.5
West	Bungo Strait	15	4	15	94.3
	Suou Nada	99	386	73	73.7
	Hibiki Nada	9	51	9	100.0
Total		795	1,017	737	92.7

Table A-4. Number of tidal flats detected by MoE and GIC in each different size

	MoE	Num. of tidal flats GIC mis-detected or didn't detect	Concordant number of tidal flats between MoE and GIC	Concordance rate
< 0.5 ha	101	100	1	1.0%
0.5 ha - 1 ha	10	10	0	0.0%
1 ha - 5 ha	451	440	11	2.4%
5 ha - 10 ha	100	94	6	6.0%
10 ha - 50 ha	110	88	22	20.0%
50 ha - 100 ha	10	4	6	60.0%
100 ha <	13	1	12	92.3%